

Instrumentation for reflectance spectroscopy and microspectroscopy with application to astrobiology

Pantazis Mouroulis, Diana L. Blaney, Robert O. Green
Jet Propulsion Laboratory, California Institute of Technology, Pasadena, CA 91109

Abstract

We present instrument concepts for in-situ reflectance spectroscopy over a spatial resolution range from several meters to tens of μm . These have been adapted to the low mass and power requirements of rover or similar platforms. Described are a miniaturized imaging spectrometer for rover mast, a combined mast and arm point spectrometer, and an imaging microspectrometer for the rover arm.

1. Introduction

Reflectance spectroscopy in the visible and short wave infrared (VSWIR) has been proven to be a valuable tool for mineral and material detection from orbiting and airborne platforms.^{1,2} On Earth there is of course abundant biological activity that can be detected and characterized through reflectance spectroscopy, while on other planetary bodies the search is for precursors or markers of past activity, especially geological evidence of the presence of water. For example, the OMEGA instrument on the Mars Express orbiter detected sulfates³ which are known to have biological potential.⁴

The success of reflectance imaging spectroscopy from orbit has not yet translated into instrumentation suitable for in-situ examination of materials. Spectroscopic instruments that have flown to date do not match the combination of data volume and diagnostic value that is available through reflectance imaging spectroscopy.

Studies of the spectral sampling and spectral range needed to resolve absorption bands in spectra and discriminate between mixtures show that the ability to identify minerals decreases dramatically at a sampling and spectrometer bandpass (Full-Width at Half-Maximum, FWHM) >20 nm, with detection difficulties beginning at ~ 15 nm.⁵ While lower resolution multi-spectral imaging can identify variation, without the full spectral information identification of specific minerals cannot normally be made. Even variation within an image can be ambiguous. For example, variations may be due to a change in abundance of clay or a change in clay mineralogy where the band center has shifted to a different wavelength.

VSWIR spectroscopy can determine mineralogy remotely with no surface preparation from a wide range of fine-grained complex mineral mixtures and is particularly advantageous for characterizing water and sulfate, carbonate and hydroxyl bonds. By contrast, determination of mineralogy in fine-grained particulates such as clays and iron oxides can be problematic with both thermal emission spectroscopy and Raman spectroscopy.⁶⁻⁸ A combination of techniques is required to cover all possible cases of

interest⁹. However, with respect to in-situ instrumentation, attention to date has concentrated on alternative techniques such as Raman or thermal emission spectroscopy, while VSWIR reflectance spectroscopy has not seen the development of viable instrument concepts despite its obvious utility.

We present below three instrument concepts that are intended to bridge the gap between remote sensing and in situ observations for reflectance spectroscopy, and provide a range of options for in situ platforms. Investigations that can be undertaken with these instruments include:

- Determination of the mineralogy and structural relationships between materials in situ at the spatial scales that characterize aqueous processes to understand the relative time and duration of water on Mars,
- Identification of materials most likely to provide direct answers to the issue of habitability for further detailed chemical analysis to assess biological potential,
- Identification of potential mineralogical biosignatures in rocks at the microscopic scale,
- Support for modeling of past climate and geological processes as derived from an investigation of the constituents of rocks and soils coupled with their spatial distribution,
- Measurement of the surface and the atmosphere at a variety of spatial and temporal scales to provide ground truth for orbital data.

2. A mast-mounted, compact imaging spectrometer

The success of the Moon Mineralogy Mapper (M3)¹⁰ instrument (due for launch on board Chandrayaan 1 in 2008) in achieving a full-range imaging spectrometer (400-3000 nm) with a total mass of ~8kg, led us to investigate whether further reductions in size were possible that would make the instrument suitable for mast-mounting, but without sacrificing the excellent uniformity of response achieved by M3.

The optical design is shown in Figure 1 (compared to the M3 optical design). The system operates at F/3.5 and has the same spectral resolution, slit and detector array as M3 but wider field of view (36°), with a nominal spatial resolution of 1mrad per pixel. The spectrometer covers the 400–2600 nm spectral region in first order with 10 nm spectral sampling. This is accomplished through a specially designed structured groove grating with optimum broadband efficiency in the first order, similar to that implemented on M3¹¹. The reduction in size is achieved in two ways. First, by splitting the monolithic M3 spectrometer mirror in two separate ones, additional degrees of freedom are provided which permit comparable optical correction to the larger M3 design. Second, by employing an innovative two-mirror anastigmat telescope (over the three-mirror anastigmat of M3), we achieve a wider field than M3 while simultaneously halving the number of telescope mirrors (the orientation of the input beam is more favorable, thus removing the need for the additional fold mirror used in M3). The new design is significantly smaller and lighter than the M3 design, with an estimated mass of 0.6 kg (compared with M3 optics mass at 2.0 kg). Additional mass savings will result from a smaller thermal enclosure than M3. However, the exact thermal enclosure and cooling

assembly will have to be optimized for a specific mission environment and are not a concern of this paper. A 640x480 element detector is used, with approximately 220 of the 480 available pixels used in the spectral direction.

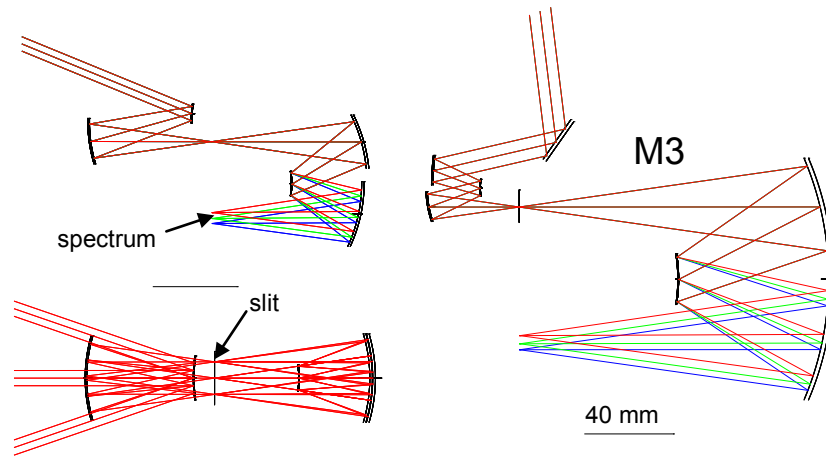


Fig. 1. M3 optical schematic (right) compared with miniaturized mast-mounted spectrometer of the same specifications (left). Top left: spectrometer in the spectral direction (y-z plane), bottom left: the spatial direction showing the field of view at the front and the slit length. A 40 mm bar is shown in both cases. The two spectrometers have identical specifications (with the exception of the long wavelength end, 2600 vs. 3000 nm) and comparable performance in every respect.

The telescope images a slit which can be in the horizontal or the vertical direction, and relies on the mast elevation and azimuth mechanisms (one for coarse aiming, the other for scanning). Considering the vertical orientation as an example, and with an integration time of $< \sim 0.15$ s, the instrument can capture a full $36^\circ \times 360^\circ$ hyperspectral cube panorama (~ 850 Mpixels) in less than 16 minutes. Of course, the resulting amount of information cannot be easily transmitted to Earth (with typical transmission volumes of 250 Mbit/day from the Martian surface), hence much smaller image cubes are likely to be the norm, and significant data compression will be required. Nevertheless the importance of reflectance imaging spectroscopy is that it allows a full mineral map of a given area to be acquired in a very short time, thus preserving resources for other instruments, and also ensuring that no significant mineralogy will be accidentally missed.

The depth of field of the instrument is 4m to infinity. Over this region, the telescope spot size retains $>80\%$ of its energy inside a $27\mu\text{m}$ square pixel for all wavelengths. At a range of 2.5m, the spatial resolution is approximately halved. The computed signal to noise ratio (SNR) is shown in Fig. 2 for various levels of target reflectance. Of note is that the SNR stays relatively flat over the entire wavelength band, which results from an optimized grating response. Figure 3 shows a terrestrial analogue image, in order to appreciate the resolution and utility of the instrument. With a presumed horizontal slit orientation, the instrument would acquire the image shown in less than 1 min, with full spectroscopic information at the high SNR shown in Fig. 2. This data acquisition capability is unmatched by other techniques.

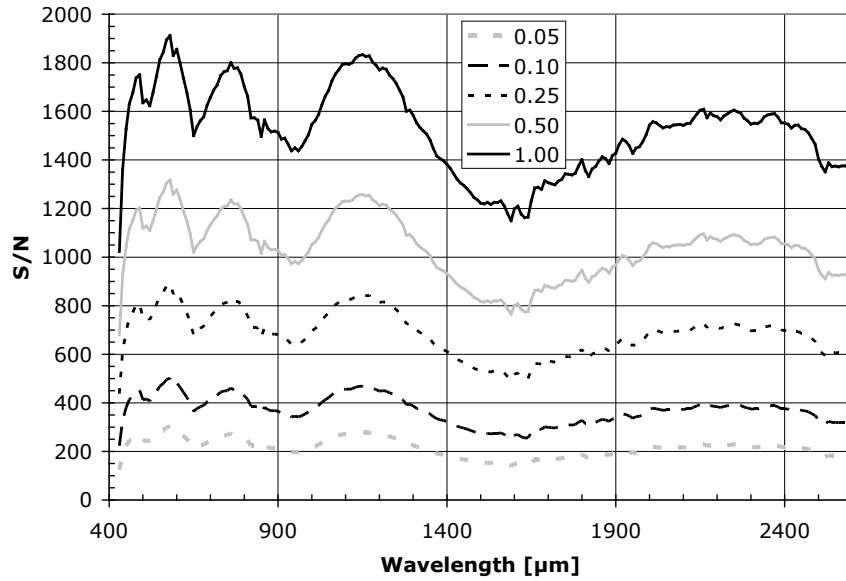


Fig. 2. Signal to noise ratio for the mast imaging spectrometer, with an integration time of 150 ms. Legend shows assumed target reflectance.

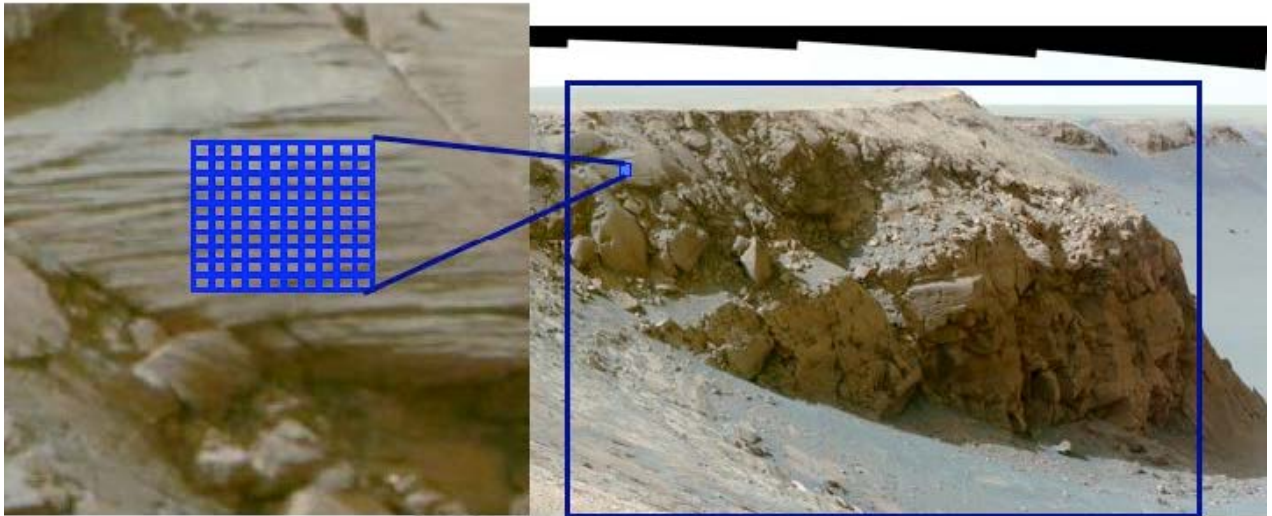


Fig. 3. Example image cube of Cape St. Mary's, Victoria Crater. The observation spans $36^{\circ} \times 20^{\circ}$ (620x344 pixels). A 10x10 pixel area is expanded showing the ability to resolve differences within layers.

3. A combined mast and arm point spectrometer

For specific missions, point spectroscopy may be preferable to imaging if the data volume cannot be handled. A point spectrometer has the potential advantage of being located remotely from the collecting optics, being connected to them through fiber optic cables. This minimizes the mass that must be carried on the mast or arm. It also allows us to combine two receiving heads on the same spectrometer, one on the mast for remote

operation and one on the arm for microscopic operation. The resulting mass savings from combining instruments operating at two very different spatial scales are significant, as is the ability to place the spectrometer and associated cooling arrangement on the rover body.

The use of an area array as a detector for the spectrometer is dictated both by heritage (similar detectors to CRISM¹² or M3) and by the desire to avoid switching mechanisms that are probably necessary with a linear array if it were to receive both signals. It also affords us the possibility to use more than a single fiber per optical head. On the other hand, a large number of fibers make the bundle stiffer and harder to qualify for flight. We have settled on four fibers from the mast head and four from the microscope head. This allows us to reduce to ~one-quarter the time it takes to cover a given area. The eight fibers form a type of slit for the spectrometer and are spaced far apart so there is no cross talk between them in the detector array.

The telescope provides a 2-mrad resolution (fiber image). It is a miniature super-achromatic lens, shown in Fig. 4 (together with the microscope optical head). The size of this “telescope”, with a total diameter of ~5mm, is essentially negligible compared with the 125 mm diameter telescope required for remote Raman spectroscopy⁷. In addition, we obtain four distinct spots instead of one.

The microscope head, also shown in Fig. 4, follows a design similar to standard dark field objectives, but is adapted to our requirements. The illumination is provided by a source (the end of a solid waveguide) placed at the focal plane of a two-mirror (Schwarzschild) reflecting objective. Light scattered from the sample is collected by the small refractive objective, at the focal plane of which are placed four imaging fibers and one confocal fiber, the function of which is to determine optimum focus according to the well-known confocal property. The confocal fiber is illuminated by a separate diode laser, not shown. The exiting fibers block only a small portion of the illumination flux. In addition to compactness, this system provides efficient illumination by imaging the source in the vicinity of the sample, thus concentrating the flux in the area of interest. The imaging objective is a miniature refractive design that is color corrected over the entire 400-2500 nm range. The transverse chromatic aberration (TCA) is only about 3 μm , negligible compared with the fiber diameter of ~100 μm . Absence of TCA is critical in avoiding spectral artifacts. The design is nearly diffraction-limited so that practically all the spot energy is contained in a circle of 15 mm radius. This means that the system resolution is still dominated by the fiber diameter. The objective is a five-element design with no cemented interfaces. The low refractive index materials used ensures high (75%) transmission even with no coatings.

The remaining of the optical system comprises a 0.75x demagnifying spectrometer system, which is required in order to maintain the spectral resolution on the detector array. In this case, the spectrum is received along 640 pixels, all of which are used.

The microscope head can scan a region 2x2mm in steps of 50-100 μm , thus creating an image that gives insight into the morphology/mineralogy of the feature under

examination. It also has a fine focus control (z-direction). The x-y motions are accomplished through a flexure mechanism, while the focus control is via a stepper motor with a guide screw and rods.

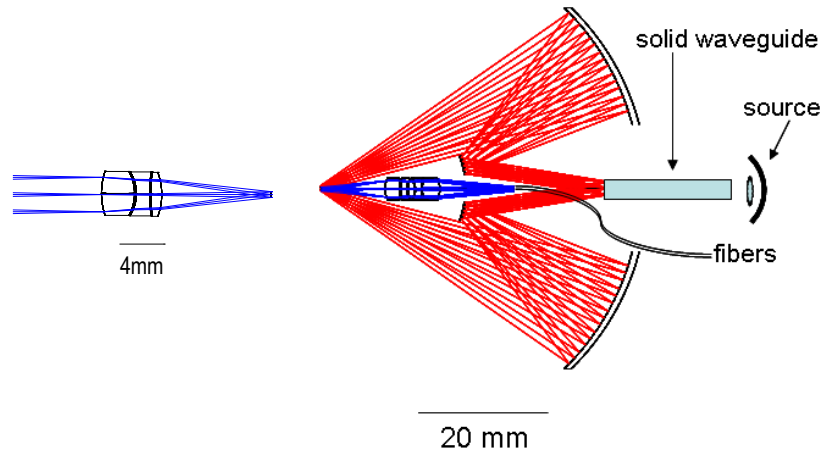


Fig. 4. Collecting optics for the combined mast and arm spectrometer. The small objective on the left is the mast “telescope”. The dark-field microscope objective on the right comprises a Schwarzschild illumination and a miniature refractive collector inside the obscuration. The microscope head is scanned by its own motors. The telescope is scanned by the mast mechanism.

There has been some question in the literature whether VSWIR microspectroscopy is at all feasible or whether spectral features are suppressed at that spatial scale. We have built a benchtop microspectrometer with two resolution modes (60 and 120 μm), which has proven that spectra closely comparable to bulk/remotely sensed ones can be obtained in dark field mode, and that the spectral signal arises from the resolved spot and not the surround. Example spectra are shown in Fig. 5, next to bulk spectra from the USGS database.¹³

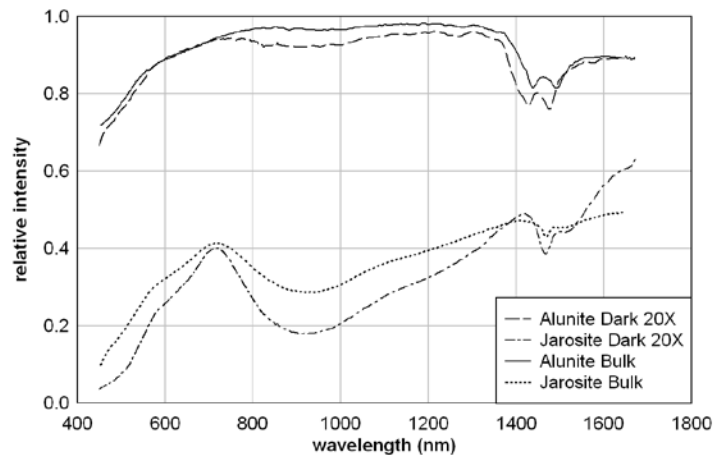


Fig. 5. Example microscopic spectra of jarosite and alunite compared with bulk. The bulk spectra have been multiplied by an arbitrary factor to account for reflectivity difference between microscopic and bulk spectra. Microscopic spectra cannot provide absolute reflectivity if derived from unprepared, rough samples.

The SNR of the mast portion is shown in Fig. 6, assuming an integration time of 20 ms. The corresponding microscope SNR depends critically on the details of the illumination. With the efficient illumination scheme shown previously, it is possible to reach similar SNR as that of Fig. 6 with comparable integration times.

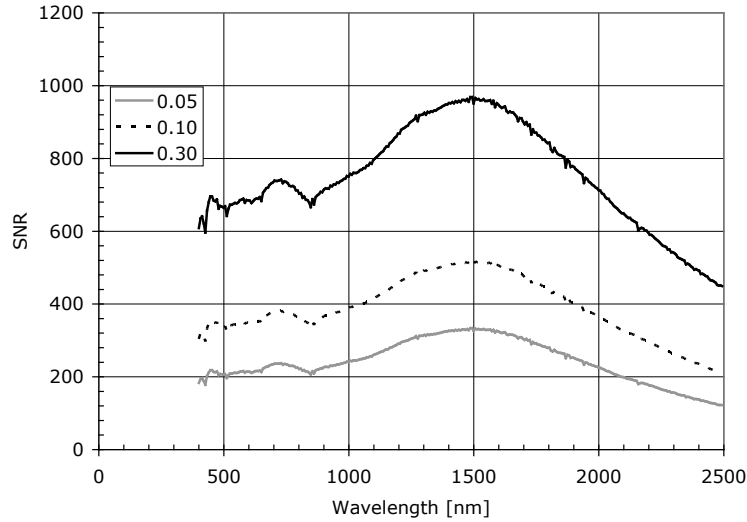


Fig. 6. Signal to noise ratio for the mast point spectrometer. The legend shows assumed object reflectance.

4. A miniature imaging microspectrometer

Using newly available thermoelectrically cooled HgCdTe detectors, it is possible to reduce the total mass of an imaging microspectrometer to the point where it can be accommodated on the arm (minus electronics). Such a spectrometer has the advantage of producing a well-registered and sampled image of a rough (or roughly abraded) rock sample. The available detector array is has 320x256 pixels of 30 μm size. The remaining specifications are summarized in Table 1.

Table 1: Specifications of imaging microspectrometer

Parameter	Value
Spectral range	800-2500 nm
Spectral sampling	9 nm
Spatial resolution at target	75 mm
# of spatial elements (swath)	320 (2.4 cm)
working distance	8 cm
depth of field	2 mm
detector type	TE-cooled HgCdTe
detector format	320 x 256 (30 μm pixel)
integration time (typ.)	0.1 s

The design is shown in Fig. 7. A miniature three-mirror relay, with an additional flat scan mirror, projects the 9.6mm long x 30 μm wide spectrometer slit onto a 24 mm x 75 μm line on the sample. The line is scanned using a small motor, to cover a desired area up to a maximum of 24 mm (corresponding to approximately 9° of mirror rotation). The relay F-number is 5 at the output (spectrometer side), and 12.5 at the input. It has been designed to provide long working distance (~8 cm). This helps with maintaining focus during the scan. As the mirror rotates, the point of best focus writes an arc, however, the sag of the arc (~1 mm) remains well within the depth of field of the relay (~2 mm). Thus the instrument does not lose focus during the scan, assuming of course that the sample is flat and properly oriented in the first place. In practice, the useful sample area may be smaller, limited by sample roughness and the ability to orient the rover arm. Other scan techniques have been examined but are not thought to be advantageous as they require additional components or larger motor.

In terms of optical performance, the relay is fully diffraction-limited at the design focus, with ensquared energy (in 30 μm) between 84 and 95% depending on wavelength. At the extremes of the depth of field, the ensquared energy drops by about 12% relative to the maximum. Even though relatively large, the depth of field is still outside the present rover arm positioning accuracy. This can be handled in two ways, either by moving the arm and discarding out of focus data, as with the MER Microscopic Imager, or by adding a second, translational motion to the scan mirror.

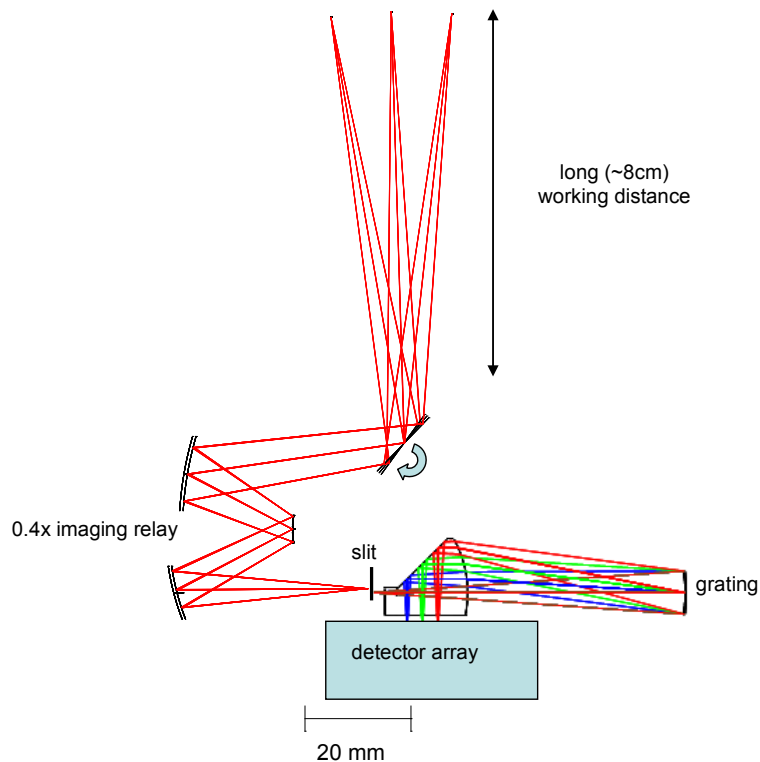


Fig. 7. A raytrace of the total system is shown, with the imaging relay at three different scan positions. The slit is perpendicular to the paper.

The scan mirror is operated by a miniature motor required to execute a scan of approximately 9° with a resolution of $\sim 1.5'$. Because the motion is always in a single direction, and because there is no need to target any specific point, backlash is not a concern, allowing simple gear reduction. Typical mirror angular speed is 0.3 deg/s. This can be achieved with a small, three-phase stepper motor, of a size $\sim 0.4''$ dia x 1.25'' long.

The heart of the instrument is a miniature spectrometer that provides 190 spectral channels over the range 800-2500 nm with a 9.6 mm long slit (320 spatial pixels). The spectrometer operates at F/5. It comprises a monolithic lens/mirror combination (with no cemented interfaces) fabricated from IR grade fused silica, and a concave reflection grating, seen in Fig. 8. Despite its simplicity and miniature size, the spectrometer optical design achieves high uniformity (orthogonality between spectral and spatial information) and small spot size. The spectrometer optical performance is summarized in Table 2. All percentages refer to a $30\ \mu\text{m}$ pixel.

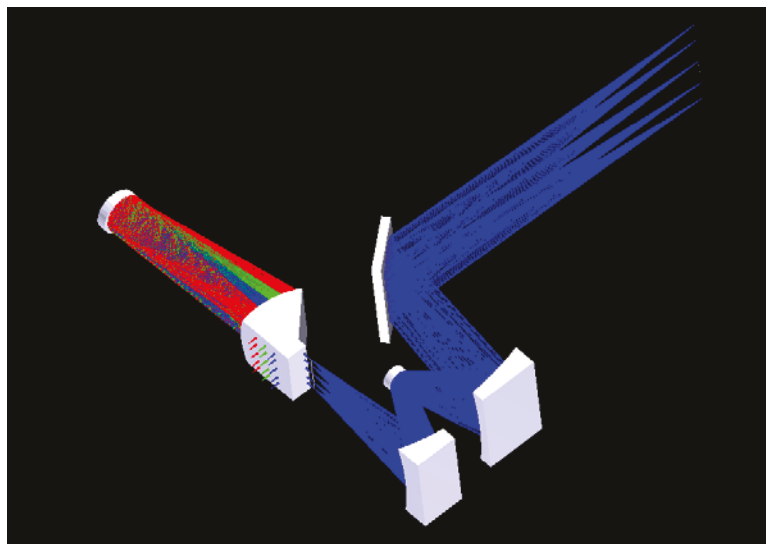


Fig. 8. Solid model of the imaging microspectrometer showing the projection of the slit onto the sample and the two-dimensional distribution of spatial and spectral information on the detector.

Table 2: Optical performance of imaging microspectrometer

Parameter	Value
Ensquared energy @ 800 nm*	92 %
Ensquared energy @ 2500 nm**	83%
Smile (fraction of pixel)	<1.5%
Keystone (fraction of pixel)	<1%

* Diffraction limited value is 95%

** Diffraction limited value is 84%

The uniformity values of a small fraction of a pixel mean that spectral artifacts are not a concern with this spectrometer and that spectral calibration will not vary with field location.¹⁴ The lack of spectral artifacts is also ensured by the use of a reflective relay, inherently free from chromatic-aberration. High uniformity values and freedom from spectral artifacts is particularly critical in a microspectroscopy experiment when attempting to recover spectra of small inclusions, where the type of spectral mixing may contain both linear and nonlinear components.¹⁵

The signal-to-noise ratio of the spectrometer has been computed to be in the 120-200 range across the entire band, assuming an integration time of 0.5 s and illumination from a distance of 10 cm with a 5W tungsten filament and no auxiliary reflectors. A single parabolic reflector behind the filament can increase the illumination by a factor of 10 or more, thus reducing the integration time to less than 0.2 s and simultaneously increasing the SNR by a factor of ~ 2 . Thus the instrument can achieve the desired SNR of over 200 while retaining a total time for one scan of less than one minute.

This instrument concept occupies a unique position among the various existing and proposed in-situ optical and analytical instruments. It is capable of imaging an area of 24 x 24mm with a resolution of 320x320 (0.1 Mpixel) while providing high-resolution, diagnostic-quality spectra of all these pixels in one minute or less, and being sufficiently lightweight to reside almost entirely on the rover arm (processing and power electronics excluded). The expected mass on the end of the arm is <1kg.

When used in conjunction with other rover capabilities, MICROExplorer can produce a wealth of data that can revolutionize in-situ observation of planetary materials at the microscopic level. It can determine spatial relations of minerals in unperturbed rocks. It is ideally suited for examining areas abraded by the rover Rock Abrasion Tool while determining the composition and distribution of inclusions within the main mineral matrix. It can determine composition of dust and ice and the constituents of dirty ice. All these capabilities are critical to understanding geological history and the biological potential of a particular site.

Although the exact limit has not been established yet, the spatial resolution of reflectance microspectroscopy is expected to be limited to structures no smaller than 10-20 μm . Biogenic structures can be much finer, requiring high-resolution microscopy for detection and morphological characterization. Reflectance microspectroscopy may still have a potential role in characterizing material abundances even if the underlying structures are spatially unresolved. However, spectral unmixing at the microscopic scale is an open area of research.

5. Conclusions

Three distinct instrument concepts have been presented that extend reflectance imaging spectroscopy capabilities to in-situ platforms. The instruments can observe and analyze surface constituents from a distance, utilizing solar reflected illumination. They can also microscopically analyze unprepared rock samples down to a resolution of 75 μm . These

instruments extend the successful orbiter observations to the in-situ domain, utilizing the same spectral signatures over spatial scales from km to tens of μm . The ability to acquire rapidly high-quality diagnostic spectra and their spatial relations from a well-registered image while retaining instrument mass under 1kg is probably unique to reflectance spectroscopy methods.

Acknowledgment

This research has been performed at the Jet Propulsion Laboratory, California Institute of Technology, under a contract with the National Aeronautics and Space Administration. We thank Hal Sobel for the SNR predictions and modeling, and Byron van Gorp for experimental work with the benchtop microspectrometer.

References

1. R. O. Green, M. L. Eastwood, C. M. Sarture, T. G. Chrien, M. Aronsson, B. J. Chippendale, J. A. Faust, B. E. Pavri, C. J. Chovit, M. Solis, M. R. Olah, and O. Williams, "Imaging spectroscopy and the Airborne Visible/Infrared Imaging Spectrometer (AVIRIS)", *Remote Sens. Environ.* **65**, 227–248 (1998)
2. R. N. Clark, G. A. Swayze, K. E. Livo, R. F. Kokaly, S. J. Sutley, J. B. Dalton, R. R. McDougal, and C. A. Gent: "Imaging spectroscopy: Earth and planetary remote sensing with the USGS Tetracorder and expert systems," *J. Geophys. Res.*, **108** (E12) 5131 (2003)
3. A. Gendrin, N. Mangold, J.-P. Bibring, Y. Langevin, B. Gondet, F. Poulet, G. Bonello, C. Quantin, J. Mustard, R. Arvidson, S. LeMouélic: "Sulfates in Martian layered terrains: the OMEGA/Mars Express view", *Science* **307**, 1587 – 1591 (2005)
4. J. L. Bishop, M. Darby, M. D. Lane, and J. F. Banfield: "Spectral identification of hydrated sulfates on Mars and comparison with acidic environments on Earth" *Int. J. Astrobiology* **3**, 275-285 (2004)
5. G. A. Swayze, R. N. Clark, A. F. H. Goetz, T. G. Chrien, and N. S. Gorelick: "Effects of spectrometer band pass, sampling, and signal-to-noise ratio on spectral identification using the Tetracorder algorithm," *J. Geophys. Res. (Planets)*, **108**:E9, 5105 (2003)
6. J. L. Bishop and E. Murad: "Characterization of minerals and biogeochemical markers on Mars: A Raman and IR spectroscopy study of montmorillonite," *J. Raman Spectr.* **35**, 480-486 (2004)
7. S. K. Sharma, P. G. Lucey, M. Ghosh, H. W. Hubble, and K. A. Horton: "Stand-off Raman spectroscopic detection of minerals on planetary surfaces," *Spectrochim. Acta* **59**, 2391-2407 (2003)

8. E. J. Israel, R. E. Arvidson, A. Wang, J. D. Pasteris, B. L. Jolliff : “Laser Raman spectroscopy of varnished basalt and implications for in situ measurements of Martian rocks,” *J. Geophys. Res. (Planets)* **102** (E12), 28705-28716 (1997)
9. J. L. Bishop, E. Murad, M. D. Lane, and R. L. Mancinelli: “Multiple techniques for mineral identification on Mars: a study of hydrothermal rocks as potential analogues for astrobiology sites on Mars,” *Icarus*, **169**, 311-323 (2004)
10. R. O. Green, C. Pieters, P. Mouroulis, and T. Koch: “The Moon Mineralogy Mapper imaging spectrometer: Science measurement characteristics and laboratory calibration results”, *IEEE Aerospace Conference*, pp. 1-5 (2008)
11. P. Mouroulis, R. G. Sellar, D. W. Wilson, J. J. Shea, and R. O. Green: “Optical design of a compact imaging spectrometer for planetary mineralogy”, *Opt. Eng.* **46** 063001 (2007)
12. S. L. Murchie and 42 co-authors: “CRISM (Compact Reconnaissance Imaging Spectrometer for Mars) on MRO (Mars Reconnaissance Orbiter)” in *Instruments, Science, and Methods for Geospace and Planetary Remote Sensing*, *SPIE Proc.* **5660**, 66-77 (2004)
13. R. N. Clark, G. A. Swayze, R. Wise, E. Livo, T. Hoefen, R. Kokaly, S. J. Sutley, USGS digital spectral library splib06a: U.S. Geological Survey, Digital Data Series 231. <http://speclab.cr.usgs.gov/spectral-lib.html> (2007)
14. P. Mouroulis, R. O. Green, and T. G. Chrien: “Design of pushbroom imaging spectrometers for optimum recovery of spectroscopic and spatial information”, *Appl. Opt.* **39**, 2210-2220 (2000)
15. R. N. Clark, “Spectroscopy of Rocks and Minerals, and Principles of Spectroscopy” Ch. 1 in *Manual of Remote Sensing, Volume 3, Remote Sensing for the Earth Sciences*, A.N. Rencz, Ed., John Wiley and Sons, New York, 1999